HHS Public Access

Author manuscript

Mol Cell. Author manuscript; available in PMC 2017 April 07.

Published in final edited form as:

Mol Cell. 2016 April 7; 62(1): 121–136. doi:10.1016/j.molcel.2016.02.005.

System-wide modulation of HECT E3 ligases with selective ubiquitin variant probes

Wei Zhang[1,12], **Kuen-Phon Wu**[2,12], **Maria A. Sartori**[1], **Hari B. Kamadurai**[2,13], **Alban Ordureau**[3], **Chong Jiang**[4], **Peter Y. Mercredi**[2], **Ryan Murchie**[4], **Jicheng Hu**[5], **Avinash Persaud**[4], **Manjeet Mukherjee**[2,14], **Nan Li**[6], **Anne Doye**[7], **John R. Walker**[5], **Yi Sheng**[8], **Zhenyue Hao**[9], **Yanjun Li**[5], **Kevin R. Brown**[1], **Emmanuel Lemichez**[7], **Junjie Chen**[6], **Yufeng Tong**[5,10], **J. Wade Harper**[3], **Jason Moffat**[1,11,15], **Daniela Rotin**[4,15], **Brenda A. Schulman**[2,15,*], and **Sachdev S. Sidhu**[1,11,15,*]

[1]Donnelly Centre for Cellular and Biomolecular Research, Banting and Best Department of Medical Research, University of Toronto, 160 College Street, Toronto, Ontario M5S3E1, Canada

[2]Department of Structural Biology and Tumor Cell Biology, Howard Hughes Medical Institute, St. Jude Children's Research Hospital, Memphis, TN 38105, USA

[3]Department of Cell Biology, Harvard Medical School, Boston, MA 02115, USA

[4]Program in Cell Biology, Hospital for Sick Children, and Department of Biochemistry, University of Toronto, Toronto, Ontario M5G 0A4, Canada

[5]Structural Genomics Consortium, University of Toronto, Toronto, Ontario M5G1L7, Canada

[6]Department of Experimental Radiation Oncology, The University of Texas MD Anderson Cancer Center, 1515 Holcombe Boulevard, Houston, Texas 77030, USA

[7]Inserm U1065, Centre Méditerranéen de Médecine Moléculaire, C3M, Equipe Labellisée La Ligue Contre Le Cancer, Université de Nice-Sophia Antipolis, 151 Route St Antoine de Ginestière, BP 2 3194, 06204 Nice Cedex, France

[8]Department of Biology, York University, Toronto, Ontario M3J1P3, Canada

[*]To whom correspondence should be addressed. brenda.schulman@stjude.org (B.A.S.) and sachdev.sidhu@utoronto.ca (S.S.S).

[12]Co-first author

[13]Present address: Biogen, 161 First Street, Cambridge, MA 02142 USA

[14]Present address: Department of Molecular and Cell Biology, University of Leicester, Leicester, LE19HN, UK

[15]Co-senior author

Full details of experimental procedures are given in Supplemental Information.

AUTHOR CONTRIBUTIONS

Conceptualization, W.Z., K.P.W., B.A.S., S.S.S.; Methodology, W.Z., K.P.W., B.A.S., S.S.S.; Software, K.R.B. and J.M.; Investigation, W.Z., K.P.W., M.A.S., H.B.K., A.O., C.J., P.Y.M., R.M., J.H., A.P. M.M., N.L., A.D., J.R.W., Y.S., Z.H, Y.L., Y.T.,; Writing – Original Draft and reviewing, W.Z., K.P.W., B.A.S., S.S.S.; Writing – Editing, E.L., J.M. and D.R.; Funding Acquisition, J.W.H., J.M., D.R., B.A.S., and S.S.S.; Supervision, E.L., J.C., Y.T., J.W.H., J.M., D.R., B.A.S., and S.S.S.

No conflicts of interest declared.

[9]Campbell Family Cancer Research Institute, University Health Network, Toronto, Ontario M5G2C1, Canada

[10]Department of Pharmacology and Toxicology, University of Toronto, Toronto, Ontario M5G1L7, Canada

[11]Department of Molecular Genetics, University of Toronto, 1 King's College Cir, Toronto, Ontario M5S1A8, Canada

SUMMARY

HECT-family E3 ligases ubiquitinate protein substrates to control virtually every eukaryotic process, and are misregulated in numerous diseases. Nonetheless, understanding of HECT E3s is limited by a paucity of selective and potent modulators. To overcome this challenge, we systematically developed ubiquitin variants (UbVs) that inhibit or activate HECT E3s. Structural analysis of 6 HECT-UbV complexes revealed UbV inhibitors hijacking the E2-binding site, and activators occupying a ubiquitin-binding exosite. Furthermore, UbVs unearthed distinct regulation mechanisms among NEDD4 subfamily HECTs and proved useful for modulating therapeutically relevant targets of HECT E3s in cells and intestinal organoids, and in a genetic screen that identified a role for NEDD4L in regulating cell migration. Our work demonstrates versatility of UbVs for modulating activity across an E3 family, defines mechanisms and provides a toolkit for probing functions of HECT E3s, and establishes a general strategy for systematic development of modulators targeting families of signaling proteins.

INTRODUCTION

Ubiquitination mediated by E1-E2-E3 multi-enzyme cascades rivals phosphorylation as a predominant mechanism regulating myriad protein functions (Cohen and Tcherpakov, 2010; Nalepa et al., 2006). Repeated catalytic cycles result in substrates modified on multiple lysines with various polyubiquitin chains, which alter protein functions in an extraordinary variety of ways. Because E3 ligases control substrate specificity and the topology of ubiquitination, they represent attractive targets for therapeutic intervention (Nalepa et al., 2006; Petroski, 2008). Yet, identifying the diversity of mechanisms regulating E3 ligases, as well as generation of tools for their manipulation, has lagged behind deciphering regulation and developing therapeutics for kinases (Cohen and Tcherpakov, 2010; Nalepa et al., 2006). Being the first family of E3 ligases discovered (Huibregtse et al., 1995), HECT (Homologous to E6AP C-Terminus) E3s are directly implicated in cancer, hypertension, neurological disorders and other diseases (Table S1) (Rotin and Kumar, 2009; Scheffner and Kumar, 2014). Moreover, some pathogenic bacteria have evolved HECT-like E3s as virulence factors to manipulate host cell signaling (Lin et al., 2012; Rohde et al., 2007). Therefore, understanding molecular mechanisms of HECT E3 function could greatly advance therapeutic strategies for many diseases.

However, development of agents to selectively modulate HECT E3s has been hampered by extreme inter-domain rotations accompanying catalysis, a shallow active site, and dynamic regulation of HECT E3 activity (Escobedo et al., 2014; Gallagher et al., 2006; Huang et al., 1999; Kamadurai et al., 2013; Kamadurai et al., 2009; Mari et al., 2014; Persaud et al., 2014;

Ronchi et al., 2013; Verdecia et al., 2003; Wiesner et al., 2007). In principle, recently reported small molecule and peptide inhibitors obtained by high throughput screening for several HECT E3s provide routes to assess functions and mechanisms of HECT E3s in normal and diseased cells (Cao et al., 2014; Kathman et al., 2015; Mund et al., 2014; Rossi et al., 2014). However, existing molecules generally do not conform to a general strategy that could be used to interrogate HECT E3s across the family, fall short in terms of potency and specificity, and generally have had limited utility in probing unknown HECT mechanisms. Thus, we sought to develop a protein-based toolkit for HECT E3s on a system-wide scale, with the goal to discover and alter unknown functions and to validate therapeutic targets supported by genetic studies.

The defining feature of HECT E3s is a ~40 kDa C-terminal "HECT domain" containing two flexibly-tethered lobes (N- and C-), with 16–92% amino acid identity across the family. In addition to the catalytic domain, HECT E3 primary sequences reveal various N-terminal domains that presumably enable substrate binding and dynamic regulation by mediating autoinhibition and influencing subcellular localization (Figure 1A). The largest and best-characterized class of HECT E3s comprises the NEDD4-family, which display a common architecture consisting of an N-terminal C2 domain, 2–4 central WW-domains distal and proximal to the catalytic domain, and the C-terminal HECT domain (Rotin and Kumar, 2009; Scheffner and Kumar, 2014) (Figure 1A).

Notably, studies of E3s in the NEDD4-family revealed that the HECT domain interacts with Ub at multiple sites. For example, in complex with E2~Ub or in the E3~Ub intermediate, the HECT "C-lobe" binds the Ub to be transferred, and a separate C-lobe interaction with the acceptor Ub is implied from biochemical studies (Kamadurai et al., 2013; Kamadurai et al., 2009; Kim and Huibregtse, 2009; Maspero et al., 2013) (Figure S1A–B). In addition to interactions made by the active-site-bound Ub, a weak Ub-binding "exosite" has been reported in the HECT "N-lobe" of various NEDD4-family E3s (French et al., 2009; Kim et al., 2011; Maspero et al., 2011; Ogunjimi et al., 2010). The diversity of Ub interactions with HECT E3s is reminiscent of deubiquitinases (DUBs), for which we recently devised a strategy to generate specific and potent inhibitors that we proposed would be adaptable to virtually any Ub-interacting protein (Ernst et al., 2013).

Our approach is based on the fact that numerous proteins that interact with Ub recognize a common surface with low affinity. The weak interactions may be required because Ub has to be quickly released after an enzymatic reaction or transient recognition has occurred. We reasoned that it is possible to identify specific mutations in Ub that produce a Ub variant (UbV) with optimized contacts to a particular Ub-interacting protein. To date, this strategy has been used to create potent and specific inhibitors that block DUB binding sites for substrate Ub molecules (Ernst et al., 2013; Phillips et al., 2013; Zhang et al., 2013). In an initial screen, we identified a UbV that bound weakly to the HECT domain of NEDD4 and acted as an activator rather than inhibitor of enzymatic function (Ernst et al., 2013). This surprising result led us to hypothesize that the inherent complexities of the HECT catalytic mechanism, involving allosteric changes and multiple Ub-binding sites, may prove advantageous to enabling the development of UbV modulators that could alter enzymatic activities to promote cellular phenotypes beyond those possible with simple active-site

inhibitors (Figure 1B). In principle, such modulators could shed light on the mechanistic subtleties and biological functions of HECT family members and could aid development of therapeutic strategies based on activation of ligase activity. Thus, we conducted a system-wide, unbiased screen with a diverse UbV library (Figure 1C–D) to explore the full potential for modulating enzyme function across the human HECT family.

RESULTS

Development of potent and selective UbV modulators for 20 HECT E3 ligases

We used a phage-displayed UbV library that varies almost all residues contacting the N-lobe exosite but only a subset of those mediating interactions in the transient catalytic intermediates (Figure S1A–C). Binding selections (Figure 1D) against purified HECT domains for 19 of 28 total human and 1 of 5 total yeast HECT E3s (Table S1) yielded 69 UbVs with a variety of substitutions across the binding surface (Tables S2). Assessment of affinities for cognate HECT domains by measuring EC50 values (Table S3 and Figure S2A) confirmed higher affinity interactions for UbVs (in some cases EC50 <10 nM) than for Ub, which in accordance with previous studies showed no detectable binding even at micromolar concentrations. Tight binding was also confirmed by Bio-Layer Interferometry (BLI) (Figures 1E–F). Indeed, many UbVs bound their cognate HECT domains 500–1000-fold tighter than Ub (Table S4 and Figure S2B–J). Moreover, ELISAs revealed that the UbVs are highly specific, as most recognize preferentially their cognate HECT domain amongst a panel of 20 HECT domains and other control proteins (Figure 1G). Even among the 9 most closely related HECT E3s in humans that comprise the NEDD4-family, for those related by ≤55% identity there was strong specificity, for example an average of 500-fold lower affinity for half the NEDD4L-binding UbVs toward WWP1 (52% identity) and 70-fold lower affinity of WWP1-binding UbVs toward NEDD4L (Figure 1F). Although there is some cross-reactivity for HECT domains that are ≥80% identical (e.g. WWP2 UbVs to WWP1), four NEDD4L-binding UbVs displayed ≥14-fold selectivity over NEDD4 (Table S4 and Figure S2B–J). While a subset of UbVs selected with WWP2 showed cross-reactivity to its close homolog WWP1, those selected with NEDD4 and WWP1 were strikingly specific and did not cross-react with non-cognate E3s sharing > 80% identity (Figure 1G–H).

Whereas previous studies confirmed that DUB catalytic activity is potently inhibited by associated UbVs targeting their substrate-binding sites (Ernst et al., 2013; Phillips et al., 2013; Zhang et al., 2013), we hypothesized that UbVs targeting different sites on HECT E3s may modulate ligase activity in a variety of ways that might not involve the active site (Figure 1B). To explore how UbVs could influence intrinsic HECT ligase enzyme activity, we monitored E3 autoubiquitination and observed a wide range of effects for 65 UbVs assayed with 20 HECT E3s (Figure 2). Indeed, many UbVs acted as inhibitors (e.g. WWP1 UbVs in Figure 2C) but others massively increased ubiquitination (e.g. WWP2 UbVs in Figure 2D). Unexpectedly, rather than having a switch-like activating or inhibiting effect, two UbVs that bind NEDD4L (NL.1 and NL.2) primarily altered extent of autoubiquitination in our assays (Figure 2B).

UbV inhibitors hijack the E2 binding site

To gain insights into the basis for specific interactions and the mechanisms whereby UbVs inhibit, activate or modulate activity, we attempted co-crystallization of numerous HECT domain-UbV complexes, with or without E2s. We focused on members of the NEDD4-family because they regulate crucial physiological processes ranging from blood pressure to immunity, their catalytic mechanisms are better characterized than those of other HECT E3s (Scheffner and Kumar, 2014), and their UbVs displayed a perplexing variety of effects despite the perceived common catalytic mechanism across this subfamily (Figure 2). We determined structures of six complexes (Table 1) that span a wide range of affinities with five different HECT domains (NEDD4L-NL.1 – 10 nM, Rsp5-R5.4 – 125 nM, WWP1-P2.3 – 230 nM, WWP1-P1.1 – 325 nM, ITCH-IT.2 – ≈10 μM and NEDD4-N4.4 – ≈90 μM) (Table S4 and Figure S2B–J), and that display inhibitory (P1.1, IT.2), activating (P2.3, N4.4) or modulatory (NL.1, R5.4) effects in autoubiquination assays, including a complex between WWP1 and a tightly binding UbV (P2.3) selected to bind the closely related WWP2. In all of the structures, UbV binding was mediated by surface contacts corresponding to Ub's classic protein interacting hydrophobic patch (positions 8, 44, 68 and 70). Furthermore, all these HECT domains displayed one of two distinctive UbV binding modes described in detail below.

Unexpectedly, UbV P1.1 on WWP1 and UbV IT.2 on ITCH inhibit not by binding a known Ub-binding site, but rather, by occupying the E2-binding site (Huang et al., 1999), which appears to be partially mobile based on the variety of conformations observed in previous structures of WWP1, ITCH, and other HECT domains (Figure 3A, Figure S1D–I). Here, UbV blocks the E2 binding site, through hydrophobic patch residues 8, 44, 68 and 70 hijacking the classic HECT E3 binding site for E2 loops 1 and 2 (F63 and P97, respectively, in a HECT-bound UBCH7) (Huang et al., 1999; Kamadurai et al., 2009) (Figure 3B). The inhibitory interactions are stabilized by numerous additional contacts, including a UbV's β1/β2 loop inserting into a nearby flexible pocket (Figure S3A–E). Accordingly, these UbVs inhibited HECT E3 activity by counteracting Ub transfer from E2 to E3 (Figures 2C, 2E and 3C–D).

N-lobe exosite bound UbVs promote E3 catalytic activities

The other four structures showed UbVs binding the N-lobe exosite of NEDD4, NEDD4L, WWP1 or Rsp5 in a manner resembling the previously described binding of Ub at this site (Kim et al., 2011; Maspero et al., 2011) (Figure 4A). The HECT domain N-lobe-Ub/UbV complexes superimpose with 0.8–1.5 Å RMSD overall, but also reveal details for how subtle differences can be exploited for specific noncovalent targeting at this site (Figure S1G and S4A–B). Although previous mutagenesis studies probed roles of Ub binding to the N-lobe exosite, the interpretations have been inconclusive and controversial. Proposed functions have ranged from competition of Ub with the C2 domain to relieve E3 autoinhibition, binding of the acceptor Ub that receives Ub from the HECT active site, or binding of substrate-linked Ub chains to either stimulate or inhibit further chain elongation (French et al., 2009; Herrador et al., 2013; Kathman et al., 2015; Kim et al., 2011; Maspero et al., 2011; Ogunjimi et al., 2010). To date, it has not been possible to differentiate positive and negative roles of exosite Ub binding with deleterious mutations. By contrast, adding a UbV to the

ubiquitination reaction can promote positive allosteric effects on the E3 while competing with prospective ubiquitinated substrates.

We therefore tested whether the NEDD4-family N-lobe exosite generally recruits an acceptor Ub and/or relieves allosteric autoinhibition mediated by the C2 domain. For NEDD4L and WWP1, we used pulse-chase assays that produce free Ub~Ub chains to monitor Ub transfer from the E3 to an acceptor Ub. Because rapid HECT E3 autoubiquitination precludes generation of stable HECT~Ub intermediates, we initiated the reactions with thioester-bonded E2~Ub intermediates for the E2 UBCH7 using a fluorescently-labeled version of Ub. Adding the E2~Ub to an active HECT E3 along with or without excess free Ub and substrate tests the effects of UbVs on E3-mediated Ub transfer from E2 to E3 to substrate or to acceptor Ub. The reactions generate a thioester-bonded E3~Ub, isopeptide-linked Ub~Ub or ubiquitinated substrate product readily detected by SDS-PAGE (Figures 4B–F and 5A–C). Surprisingly, experiments performed in the presence of UbVs excluded some previously hypothesized roles and instead identified novel functions for this exosite on NEDD4L and WWP1. Saturating the N-lobe exosite with a UbV did not inhibit Ub~Ub synthesis, ruling out the possibility that this site binds the acceptor Ub. Unexpectedly, these UbVs *activated* E3~Ub, Ub~Ub synthesis and substrate ubiquitination for multiple truncation mutants of both E3s, suggesting that the UbVs allosterically activate through mechanisms not involving the C2 domain (Figures 4D–F and 5A–C). Notably, occupation of the N-lobe exosite by a UbV has different effects on different HECT E3s, because all versions of WWP1 including the isolated HECT domain showed substantially activated Ub~Ub synthesis whereas inclusion of distal WW domains was required to observe dramatic UbV-mediated activation for NEDD4L (Figures 4E versus 5B).

To further probe how UbVs differentially modulate HECT E3 activities, we performed a battery of experiments with various substrates using either WT Ub or methylated Ub that cannot form chains (Figures 5D-5F, S5, and S6). Taken together, our data imply that UbV occupation of the N-lobe exosite modulates activity through numerous mechanisms that were not previously reported. For example, for NEDD4L and Rsp5, N-lobe exosite-binding UbVs activated the transthioesterification reaction (Ub transfer from E2 to E3) in a manner that is independent of the C2 domain but depends on the distal WW domains, presumably by relieving their autoinhibition (Figures 4D, 4F, 5D–F, and S5B) (Riling et al., 2015). Intriguingly, two UbVs modulate NEDD4L activity by decreasing processive and increasing distributive multi-monoUb ligation directly to substrate, with slightly increased Ub chain elongation (Figure S6A–E and H–I). Thus, unlike previous reports on other NEDD4-family members that suggested blocking Ub binding primarily inhibits processive extension of a Ub chain (Kathman et al., 2015; Kim et al., 2011; Maspero et al., 2011; Maspero et al., 2013), our data demonstrate that occupation of the exosite positively and negatively influences many properties of the reaction. Accordingly, ubiquitination can be activated by relief from autoinhibition and increased substrate turnover, yet individual substrate molecules may have fewer lysines modified at a time. Depending on reaction conditions, there may be increased flux through the pathway when NEDD4L is saturated with an exosite-binding UbV. Indeed, we used the UB-AQUA method, an unbiased proteomics approach for quantifying ubiquitin signaling (Kirkpatrick et al., 2005; Ordureau et al., 2015; Ordureau et al., 2014; Phu et al., 2011), and found that NL.1 increased the total abundance of Ub chains, primarily containing

canonical K63-linkages, formed on *in vitro* autoubiquitinated NEDD4L (Figure 4G–I). Furthermore, this effect was also observed upon induction of NL.1 expression in HEK293 cells, which resulted in a ~20% increase in total K63-linked chains (Figure 4J).

Interestingly, the effect of UbV binding to the N-lobe exosite on WWP1 differs from the effect on NEDD4L (Figures 5D–G and S6). Although UbV P2.3 slightly inhibits WWP1 reactions where a substrate molecule only encounters the E3 once, it massively increases the amount of substrate modified and the number of Ubs attached in reactions where ubiquitinated products that are released can re-bind WWP1 in numerous reaction cycles (Figure S6F, G, J). The simplest interpretation is that UbVs block capture of a substrate-linked Ub and that this is less important for processive monoubiquitination of multiple sites during a single encounter with WWP1 than with NEDD4L. Instead, our data are consistent with a model where this is more important for reactions where ubiquitinated substrates come off and on E3s during repeated reaction cycles (Figure S6B–E vs. F–G).

UbVs modulate HECT E3 functions in cells and intestinal organoids (mini-guts)

Given the utility of the UbVs for probing HECT E3 functions *in vitro*, and the parallel effects of UbV NL.1 on increasing Ub chain formation in mammalian cells (Figure 4J), we examined effects in cells upon expressing UbVs targeting a select panel of HECT E3s (HACE1, HUWE1, WWP2, and NEDD4L). In all cases, expression of UbVs increased or attenuated ubiquitination levels in accordance with their *in vitro* properties (Inoue et al., 2013; Maddika et al., 2011; Torrino et al., 2011). For instance, inhibitors of HACE1 or HUWE1 significantly decreased ubiquitination of the HACE1 target Rac1 (Figure S7A) or stabilized the protein levels of HUWE1 and its substrate c-Myc, respectively (Figure S7B). Furthermore, activators of WWP2 increased autoubiquitination and degradation of WWP2 and its substrate PTEN (Figure S7C–D).

We also evaluated the effects of UbVs targeting NEDD4L on regulation of its best-characterized substrate, the Epithelial Na^+ Channel, ENaC (*SCNN1*) (Kamynina et al., 2001; Kimura et al., 2011). Kidney-derived epithelial MDCK cells stably expressing αβγENaC (Figure 6A–B) and activator NL.1 or inhibitor NL.3 (Figure S7E) were tested for ENaC cell surface stability and function. Our results show reduced stability and cell-surface expression of ENaC by NL.1, but not NL.3 (Figures 6A–C and S7F), and accordingly, reduced or enhanced ENaC function (amiloride-sensitive Na^+ channel activity, Isc) by NL.1 or NL.3, respectively (Figure 6D–E). Taken together, these results show that UbVs activate or inhibit HECT E3s in cells in a manner consistent with their *in vitro* activities.

The ability to modulate NEDD4L activity is of particular interest, because elevated cell surface expression of ENaC and NCC (Na^+-Cl^- Co-transporter, another NEDD4L substrate) in the distal nephron causes increased Na^+ reabsorption and salt-induced hypertension (Ronzaud et al., 2013). Indeed, mutations in the PY motifs of ENaC, which prevent proper NEDD4L binding to and suppression of this channel, cause Liddle syndrome, a hereditary hypertension disorder (Lifton et al., 2001). Likewise, renal tubular deficiency of NEDD4L causes salt-induced hypertension by elevated NCC and ENaC abundance and function (Ronzaud et al., 2013). The increased NCC function and hypertension partially resembles Pseudohypoaldosteronism II (PHA II), another genetic hypertension caused by elevated

NCC function due to mutations in its regulators, the WNK kinases (Wilson et al., 2001). Moreover, NEDD4L targets ENaC in lung epithelia, and NEDD4L depletion there causes massive inflammation and airway mucus plugging, resembling lung disease in cystic fibrosis patients (Kimura et al., 2011).

Thus, our identification of UbV activators of NEDD4L function could point to a novel therapeutic avenue for the treatment of hypertension and inflammation. This would require a proof that UbVs can function in mammalian tissues, not just in isolated cells. To this end, we utilized the recently developed technology to grow three-dimensional intestinal epithelial organoids (mini-guts) from intestinal stem cells (Sato and Clevers, 2013) and grew mouse distal colon organoids; the distal colon strongly expresses both ENaC and NEDD4L ((Duc et al., 1994) and Jiang & Rotin, unpublished). Consistent with inhibition of ENaC function observed in MDCK cells, lentiviral transduction of NL.1 caused organoid luminal swelling due to reduced fluid reabsorption into the media, while expression of NL.3 had the opposite effect (Figures 6F and S7G). The effect of UbVs on the organoid luminal volume change is likely mediated by NEDD4L regulating ENaC (which is expressed in these organoids, Figure S7H), as treatment of NL.3 UbV-transduced organoids with the ENaC inhibitor amiloride prevents the reduction in organoid surface area (Figure 6G). In conclusion, these data suggested that activation of NEDD4L by targeting of the N-lobe exosite could be a means for treatment of hypertension and inflammation.

Lentiviral UbV genetic screen identifies novel functions of HECT E3s

To test whether UbVs can be used in a screen to discover unknown biological functions of HECT E3s in an unbiased and high-throughput manner, we used our UbV panel to globally interrogate the family for roles in cell migration, a pathway known to involve ubiquitination and that is central to embryonic development and plays a major role in cancer invasion and metastasis (Deng and Huang, 2014; Simpson et al., 2008). While SMURF2 and HACE1 have been implicated in cell migration by RNA interference studies (Castillo-Lluva et al., 2013; David et al., 2014; Jin et al., 2009), we wondered whether our unprecedented ability to activate (or block) enzyme activity with UbVs could both score these positive controls and also potentially reveal roles for other HECT E3s not known previously as regulators of this pathway. To this end, we transduced HCT116 human colon cancer carcinoma cells with a pool of 83 distinct lentiviruses, each containing an inducible defined UbV expression cassette targeting one of 19 HECT E3s or one of 13 other proteins, and analyzed the migratory response in a trans-well migration assay by deep sequencing (Figure 7A–B). Selected modulatory UbVs were further validated individually using two different cell migration assays (Figures 7C–E).

Upon induction of UbV expression by doxycycline and as expected based on RNA interference experiments (Castillo-Lluva et al., 2013; Jin et al., 2009), our screen identified inhibitors of HACE1 (HA.3) and SMURF2 (S2.5) that increased or decreased cell migration, respectively (Figure 7B). In addition, we found that two activators (P2.3 and NL.1) caused striking decreases in cell migration. UbV P2.3 binds to both WWP1 and WWP2 (Table S4), and its effect is thus likely due to the combined activation of these two enzymes. UbV NL.1 potently and specifically activates NEDD4L, which has not previously been implicated in

cell migration. To identify putative NEDD4L substrates, we assayed effects of UbV NL.1 transient expression on protein levels of small GTPases, which are key regulators of cell migration (Alfano et al., 2012; Torrino et al., 2011; Wang et al., 2003; Wang et al., 2014). Notably, we observed decreased abundance of endogenous RhoB protein following transient or inducible expression of NL.1 (Figures 7F and S7I), suggesting that RhoB could be an ubiquitination substrate of NEDD4L. Consistent with this, we observed that NEDD4L interacts with RhoB in a co-immunoprecipitation (IP) experiment (Figure 7G). Moreover, NEDD4L was able to ubiquitinate RhoB in cells (Figure 7H) and *in vitro* (Figure S7J), a process that was enhanced by NL.1. We further confirmed that in HCT116 cells, the depletion of RhoB decreased cell migration to the same level as Rac1 knockdown (Figure 7I). Although the function of RhoB in cell migration is not entirely understood, our observations are consistent with a report showing that depletion of RhoB can significantly reduce migration and invasion of prostate carcinoma cells (Alfano et al., 2012). Based on our observations, RhoB is likely functional substrate of NEDD4L in regulating cell migration and access to both inhibitors and activators of HECT E3s enhanced our view of how these enzymes work to regulate cell migration (Figure 7J). The results imply that activation of NEDD4L through binding to the N-lobe exosite could be exploited as a novel means for inhibition of metastatic phenotypes.

DISCUSSION

There is great need for platforms that enable exploring functions of entire protein families in a wide array of settings. Indeed, the ability to screen kinases with hundreds of thousands of related potential inhibitory compounds has revolutionized our understanding of phosphoregulation and has revealed phosphorylation cascades to target for therapeutic development (Gross et al., 2015; Zhang et al., 2009). Given that ubiquitination plays equally important roles in signaling pathways essential for human health (Nalepa et al., 2006), it is very likely that similar systems directed at probing E3 ligase functions will yield new therapeutic avenues for many diseases. Furthermore, while traditional screening methods typically focus on developing inhibitors, an emerging concept is that allosteric modulators are likewise useful tools for interrogating pathways and developing therapeutics (Arkin et al., 2014; Hardy and Wells, 2004).

Here we showed that engineered UbVs are broadly useful for probing various functions across an E3 ligase family. Rather than acting as simple substrate mimics that target the active site, the UbVs acted through alternative structural mechanisms, which led to many unanticipated discoveries that collectively demonstrate versatility of the platform and diversity of HECT E3 ligase mechanisms. First, UbVs can target sites not known previously to bind Ub, such as the E2-binding site. Thus, it seems that the plasticity of the Ub fold allows selection of UbVs that target binding sites in general, although the striking similarity of the WWP1 and ITCH complexes with their UbVs also raises the question as to whether Ub may bind here as a natural means of regulation. Second, the ability to use UbVs to probe functions across an E3 ligase family unveiled strikingly different roles of parallel interactions targeting HECT N-lobe exosites on different reactions performed by a given HECT E3, and among homologous proteins. Third, our system allows simultaneous selection of UbVs modulating various protein activities, showing that the complexity of

multi-domain proteins can be exploited to alter rather than inhibit enzymatic functions. Notably, we anticipate that future studies could improve capturing distinctive mechanisms, for example through addition of various types of counter-screens during UbV selection.

Because a screen for UbV binders can yield modulators targeting different sites, which lead to very different effects on enzymatic function, the options for identifying potential pathways for therapeutic intervention are expanded beyond simple inhibition. Insights gained from *in vitro* analyses can be extended to cellular systems with lentiviral delivery of UbV genes. In particular, as shown by the example of NEDD4L, activation of E3 ligases may be exploited to enhance ubiquitination and degradation of ion channels involved in the regulation of blood pressure and inflammation, and of signaling proteins involved in cell migration and other cell functions that are subverted during cancer progression. Moreover, our results with NEDD4L UbV expression in colonic mini-guts demonstrate for the first time that UbVs can function in mammalian tissues, suggesting a means for modulating HECT E3 ligase activity for therapeutic benefit, and establish utility of the system in models of development and disease. We anticipate that our UbV toolkit will be useful for researchers exploring other pathways regulated by HECT E3s in cells and tissues, and that the UbV selection platform will be generally amenable to cellular screens for studying the biology of ubiquitination and for the identification of new strategies for therapeutic targeting that go beyond traditional inhibitor development.

EXPERIMENTAL PROCEDURES

Selection of UbVs by phage display

The phage displayed UbV library used in this study was re-amplified from Library 2 as described (Ernst et al., 2013). Protein immobilization and UbV binding selections were performed according to established protocols (Tonikian et al., 2007).

Protein crystallization

Six HECT E3-UbV complexes were crystalized: NEDD4L^{HECT}-UbV NL.1, WWP1^{HECT}-UbV P2.3-UBCH7, WWP1^{HECT}-UbV P1.1, Rsp5^{HECT}-UbV R5.4, ITCH^{HECT}-UbV IT.2, and NEDD4^{HECT}-UbV N4.4. Crystallization conditions and data analysis details are in Supplemental Information.

Pulse-chase ubiquitination assays

The biochemical assays were performed and monitored using either fluorescently labeled ubiquitin (Ub*, * stands for fluorescein probe) or substrates (WBP2* or S-WBP2-1K*). In all UbV-treated assays, 10-fold molar ratio of UbV/E3 was used to saturate HECT E3 with UbV during the entire reaction time. All reacted samples were quenched by mixing with SDS sample loading buffer, separated by SDS-PAGE and analyzed based on fluorescent signals of Ub*, WBP2* or S-WBP2-1K*. A Typhoon FLA9500 Phosphoimager (GE Healthcare) was used to scan fluorescent gel images.

ENaC stability and functional assays

To evaluate ENaC cell surface stability, MDCK cells stably expressing αβγENaC (Lu et al., 2007) together with NL.1 or NL.3 were seeded on 6-well plates and treated (or not) with 44.4 μM cycloheximide (CHX) at the indicated times. Cells were biotin-labeled with 0.5 mg/ml EZ-Link Sulfo-NHS-LC-Biotin (15 min, 4 °C), washed with PBS to remove unbound biotin, and lysed. Stability of surface ENaC was determined by quantifying αENaC, as described in Supplemental Information, together with procedures for Ussing chamber analysis and Immunofluorescent (IF) confocal microscopy.

Supplementary Material

Refer to Web version on PubMed Central for supplementary material.

Acknowledgments

We thank members of the Sidhu and Schulman groups for helpful comments. We thank Andrew Vorobyov, Eva Chou, Yogesh Hooda, Jun Gu and Aiping Dong for technical assistance. We are indebted to Pankaj Garg, Andreas Ernst, Abiodun Ogunjimi, Clare Jeon, Satra Nim, Frank Sicheri and Hongrui Wang for reagents and advice. J.W.H. was supported by NIH (R37NS083524 and GM095567). A.O. was supported by an Edward R. and Anne G. Lefler Center postdoctoral fellowship. J.W.H. is a consultant for Millennium: the Takada Oncology Company and Biogen. D.R. holds a Canada Research Chair (Tier 1 in Biochemistry and Signal Transduction) and was supported by CIHR (MOP#130422). B.A.S. is an investigator of the Howard Hughes Medical Institute (HHMI) and was supported by ALSAC, NIH R37GM065930 and P30CA021765. NECAT and APS were supported by NIH P41 GM103403 and DOE Contract DE-AC02-06CH11357. W.Z. was supported by a CIHR postdoctoral fellowship. S.S.S. and J.M. were supported by CIHR (MOP#111149 and 136956). The Structural Genomics Consortium (SGC) is a registered charity (number 1097737) that receives funds from AbbVie, Bayer Pharma AG, Boehringer Ingelheim, Canada Foundation for Innovation, Eshelman Institute for Innovation, Genome Canada, Innovative Medicines Initiative (EU/EFPIA) [ULTRA-DD grant no. 115766], Janssen, Merck & Co., Novartis Pharma AG, Ontario Ministry of Economic Development and Innovation, Pfizer, São Paulo Research Foundation-FAPESP, Takeda, and the Wellcome Trust.

References

Alfano D, Ragno P, Stoppelli MP, Ridley AJ. RhoB regulates uPAR signalling. Journal of cell science. 2012; 125:2369–2380. [PubMed: 22366462]

Arkin MR, Tang Y, Wells JA. Small-molecule inhibitors of protein-protein interactions: progressing toward the reality. Chemistry & biology. 2014; 21:1102–1114. [PubMed: 25237857]

Cao Y, Wang C, Zhang X, Xing G, Lu K, Gu Y, He F, Zhang L. Selective small molecule compounds increase BMP-2 responsiveness by inhibiting Smurf1-mediated Smad1/5 degradation. Scientific reports. 2014; 4:4965. [PubMed: 24828823]

Castillo-Lluva S, Tan CT, Daugaard M, Sorensen PH, Malliri A. The tumour suppressor HACE1 controls cell migration by regulating Rac1 degradation. Oncogene. 2013; 32:1735–1742. [PubMed: 22614015]

Cohen P, Tcherpakov M. Will the ubiquitin system furnish as many drug targets as protein kinases? Cell. 2010; 143:686–693. [PubMed: 21111230]

David D, Jagadeeshan S, Hariharan R, Nair AS, Pillai RM. Smurf2 E3 ubiquitin ligase modulates proliferation and invasiveness of breast cancer cells in a CNKSR2 dependent manner. Cell division. 2014; 9:2. [PubMed: 25191523]

Deng S, Huang C. E3 ubiquitin ligases in regulating stress fiber, lamellipodium, and focal adhesion dynamics. Cell adhesion & migration. 2014; 8:49–54. [PubMed: 24589622]

Duc C, Farman N, Canessa CM, Bonvalet JP, Rossier BC. Cell-specific expression of epithelial sodium channel alpha, beta, and gamma subunits in aldosterone-responsive epithelia from the rat: localization by in situ hybridization and immunocytochemistry. The Journal of cell biology. 1994; 127:1907–1921. [PubMed: 7806569]

Ernst A, Avvakumov G, Tong J, Fan Y, Zhao Y, Alberts P, Persaud A, Walker JR, Neculai AM, Neculai D, et al. A strategy for modulation of enzymes in the ubiquitin system. Science. 2013; 339:590–595. [PubMed: 23287719]

Escobedo A, Gomes T, Aragon E, Martin-Malpartida P, Ruiz L, Macias MJ. Structural basis of the activation and degradation mechanisms of the E3 ubiquitin ligase Nedd4L. Structure. 2014; 22:1446–1457. [PubMed: 25295397]

French ME, Kretzmann BR, Hicke L. Regulation of the RSP5 ubiquitin ligase by an intrinsic ubiquitin-binding site. The Journal of biological chemistry. 2009; 284:12071–12079. [PubMed: 19252184]

Gallagher E, Gao M, Liu YC, Karin M. Activation of the E3 ubiquitin ligase Itch through a phosphorylation-induced conformational change. Proceedings of the National Academy of Sciences of the United States of America. 2006; 103:1717–1722. [PubMed: 16446428]

Gross S, Rahal R, Stransky N, Lengauer C, Hoeflich KP. Targeting cancer with kinase inhibitors. J Clin Invest. 2015; 125:1780–1789. [PubMed: 25932675]

Hardy JA, Wells JA. Searching for new allosteric sites in enzymes. Current opinion in structural biology. 2004; 14:706–715. [PubMed: 15582395]

Herrador A, Leon S, Haguenauer-Tsapis R, Vincent O. A mechanism for protein monoubiquitination dependent on a trans-acting ubiquitin-binding domain. The Journal of biological chemistry. 2013; 288:16206–16211. [PubMed: 23645667]

Huang L, Kinnucan E, Wang G, Beaudenon S, Howley PM, Huibregtse JM, Pavletich NP. Structure of an E6AP-UbcH7 complex: insights into ubiquitination by the E2–E3 enzyme cascade. Science. 1999; 286:1321–1326. [PubMed: 10558980]

Huibregtse JM, Scheffner M, Beaudenon S, Howley PM. A family of proteins structurally and functionally related to the E6-AP ubiquitin-protein ligase. Proceedings of the National Academy of Sciences of the United States of America. 1995; 92:2563–2567. [PubMed: 7708685]

Inoue S, Hao Z, Elia AJ, Cescon D, Zhou L, Silvester J, Snow B, Harris IS, Sasaki M, Li WY, et al. Mule/Huwe1/Arf-BP1 suppresses Ras-driven tumorigenesis by preventing c-Myc/Miz1-mediated down-regulation of p21 and p15. Genes & development. 2013; 27:1101–1114. [PubMed: 23699408]

Jin C, Yang YA, Anver MR, Morris N, Wang X, Zhang YE. Smad ubiquitination regulatory factor 2 promotes metastasis of breast cancer cells by enhancing migration and invasiveness. Cancer research. 2009; 69:735–740. [PubMed: 19155312]

Kamadurai HB, Qiu Y, Deng A, Harrison JS, Macdonald C, Actis M, Rodrigues P, Miller DJ, Souphron J, Lewis SM, et al. Mechanism of ubiquitin ligation and lysine prioritization by a HECT E3. eLife. 2013; 2:e00828. [PubMed: 23936628]

Kamadurai HB, Souphron J, Scott DC, Duda DM, Miller DJ, Stringer D, Piper RC, Schulman BA. Insights into ubiquitin transfer cascades from a structure of a UbcH5B approximately ubiquitin-HECT(NEDD4L) complex. Molecular cell. 2009; 36:1095–1102. [PubMed: 20064473]

Kamynina E, Tauxe C, Staub O. Distinct characteristics of two human Nedd4 proteins with respect to epithelial Na(+) channel regulation. American journal of physiology. Renal physiology. 2001; 281:F469–477. [PubMed: 11502596]

Kathman SG, Span I, Smith AT, Xu Z, Zhan J, Rosenzweig AC, Statsyuk AV. A Small Molecule That Switches a Ubiquitin Ligase From a Processive to a Distributive Enzymatic Mechanism. J Am Chem Soc. 2015

Kim HC, Huibregtse JM. Polyubiquitination by HECT E3s and the determinants of chain type specificity. Molecular and cellular biology. 2009; 29:3307–3318. [PubMed: 19364824]

Kim HC, Steffen AM, Oldham ML, Chen J, Huibregtse JM. Structure and function of a HECT domain ubiquitin-binding site. EMBO reports. 2011; 12:334–341. [PubMed: 21399621]

Kimura T, Kawabe H, Jiang C, Zhang W, Xiang YY, Lu C, Salter MW, Brose N, Lu WY, Rotin D. Deletion of the ubiquitin ligase Nedd4L in lung epithelia causes cystic fibrosis-like disease. Proceedings of the National Academy of Sciences of the United States of America. 2011; 108:3216–3221. [PubMed: 21300902]

Kirkpatrick DS, Gerber SA, Gygi SP. The absolute quantification strategy: a general procedure for the quantification of proteins and post-translational modifications. Methods. 2005; 35:265–273. [PubMed: 15722223]

Lifton RP, Gharavi AG, Geller DS. Molecular mechanisms of human hypertension. Cell. 2001; 104:545–556. [PubMed: 11239411]

Lin DY, Diao J, Chen J. Crystal structures of two bacterial HECT-like E3 ligases in complex with a human E2 reveal atomic details of pathogen-host interactions. Proceedings of the National Academy of Sciences of the United States of America. 2012; 109:1925–1930. [PubMed: 22308380]

Lu C, Pribanic S, Debonneville A, Jiang C, Rotin D. The PY motif of ENaC, mutated in Liddle syndrome, regulates channel internalization, sorting and mobilization from subapical pool. Traffic. 2007; 8:1246–1264. [PubMed: 17605762]

Maddika S, Kavela S, Rani N, Palicharla VR, Pokorny JL, Sarkaria JN, Chen J. WWP2 is an E3 ubiquitin ligase for PTEN. Nature cell biology. 2011; 13:728–733. [PubMed: 21532586]

Mari S, Ruetalo N, Maspero E, Stoffregen MC, Pasqualato S, Polo S, Wiesner S. Structural and functional framework for the autoinhibition of Nedd4-family ubiquitin ligases. Structure. 2014; 22:1639–1649. [PubMed: 25438670]

Maspero E, Mari S, Valentini E, Musacchio A, Fish A, Pasqualato S, Polo S. Structure of the HECT:ubiquitin complex and its role in ubiquitin chain elongation. EMBO reports. 2011; 12:342–349. [PubMed: 21399620]

Maspero E, Valentini E, Mari S, Cecatiello V, Soffientini P, Pasqualato S, Polo S. Structure of a ubiquitin-loaded HECT ligase reveals the molecular basis for catalytic priming. Nature structural & molecular biology. 2013; 20:696–701.

Mund T, Lewis MJ, Maslen S, Pelham HR. Peptide and small molecule inhibitors of HECT-type ubiquitin ligases. Proceedings of the National Academy of Sciences of the United States of America. 2014; 111:16736–16741. [PubMed: 25385595]

Nalepa G, Rolfe M, Harper JW. Drug discovery in the ubiquitin-proteasome system. Nature reviews. Drug discovery. 2006; 5:596–613. [PubMed: 16816840]

Ogunjimi AA, Wiesner S, Briant DJ, Varelas X, Sicheri F, Forman-Kay J, Wrana JL. The ubiquitin binding region of the Smurf HECT domain facilitates polyubiquitylation and binding of ubiquitylated substrates. The Journal of biological chemistry. 2010; 285:6308–6315. [PubMed: 20026602]

Ordureau A, Munch C, Harper JW. Quantifying ubiquitin signaling. Molecular cell. 2015; 58:660–676. [PubMed: 26000850]

Ordureau A, Sarraf SA, Duda DM, Heo JM, Jedrychowski MP, Sviderskiy VO, Olszewski JL, Koerber JT, Xie T, Beausoleil SA, et al. Quantitative proteomics reveal a feedforward mechanism for mitochondrial PARKIN translocation and ubiquitin chain synthesis. Molecular cell. 2014; 56:360–375. [PubMed: 25284222]

Persaud A, Alberts P, Mari S, Tong J, Murchie R, Maspero E, Safi F, Moran MF, Polo S, Rotin D. Tyrosine phosphorylation of NEDD4 activates its ubiquitin ligase activity. Science signaling. 2014; 7:ra95. [PubMed: 25292214]

Petroski MD. The ubiquitin system, disease, and drug discovery. BMC biochemistry. 2008; 9(Suppl 1):S7. [PubMed: 19007437]

Phillips AH, Zhang Y, Cunningham CN, Zhou L, Forrest WF, Liu PS, Steffek M, Lee J, Tam C, Helgason E, et al. Conformational dynamics control ubiquitin-deubiquitinase interactions and influence in vivo signaling. Proceedings of the National Academy of Sciences of the United States of America. 2013; 110:11379–11384. [PubMed: 23801757]

Phu L, Izrael-Tomasevic A, Matsumoto ML, Bustos D, Dynek JN, Fedorova AV, Bakalarski CE, Arnott D, Deshayes K, Dixit VM, et al. Improved quantitative mass spectrometry methods for characterizing complex ubiquitin signals. Molecular & cellular proteomics: MCP. 2011; 10 M110 003756.

Riling C, Kamadurai H, Kumar S, O'Leary CE, Wu KP, Manion EE, Ying M, Schulman BA, Oliver PM. Itch WW domains inhibit its E3 ubiquitin ligase activity by blocking E2-E3 transthiolation. The Journal of biological chemistry. 2015

Rohde JR, Breitkreutz A, Chenal A, Sansonetti PJ, Parsot C. Type III secretion effectors of the IpaH family are E3 ubiquitin ligases. Cell Host Microbe. 2007; 1:77–83. [PubMed: 18005683]

Ronchi VP, Klein JM, Haas AL. E6AP/UBE3A ubiquitin ligase harbors two E2~ubiquitin binding sites. The Journal of biological chemistry. 2013; 288:10349–10360. [PubMed: 23439649]

Ronzaud C, Loffing-Cueni D, Hausel P, Debonneville A, Malsure SR, Fowler-Jaeger N, Boase NA, Perrier R, Maillard M, Yang B, et al. Renal tubular NEDD4-2 deficiency causes NCC-mediated salt-dependent hypertension. J Clin Invest. 2013; 123:657–665. [PubMed: 23348737]

Rossi M, Rotblat B, Ansell K, Amelio I, Caraglia M, Misso G, Bernassola F, Cavasotto CN, Knight RA, Ciechanover A, et al. High throughput screening for inhibitors of the HECT ubiquitin E3 ligase ITCH identifies antidepressant drugs as regulators of autophagy. Cell death & disease. 2014; 5:e1203. [PubMed: 24787015]

Rotin D, Kumar S. Physiological functions of the HECT family of ubiquitin ligases. Nature reviews. Molecular cell biology. 2009; 10:398–409. [PubMed: 19436320]

Sato T, Clevers H. Growing self-organizing mini-guts from a single intestinal stem cell: mechanism and applications. Science. 2013; 340:1190–1194. [PubMed: 23744940]

Scheffner M, Kumar S. Mammalian HECT ubiquitin-protein ligases: biological and pathophysiological aspects. Biochimica et biophysica acta. 2014; 1843:61–74. [PubMed: 23545411]

Sheng Y, Hong JH, Doherty R, Srikumar T, Shloush J, Avvakumov GV, Walker JR, Xue S, Neculai D, Wan JW, et al. A human ubiquitin conjugating enzyme (E2)-HECT E3 ligase structure-function screen. Molecular & cellular proteomics: MCP. 2012; 11:329–341. [PubMed: 22496338]

Simpson KJ, Selfors LM, Bui J, Reynolds A, Leake D, Khvorova A, Brugge JS. Identification of genes that regulate epithelial cell migration using an siRNA screening approach. Nature cell biology. 2008; 10:1027–1038. [PubMed: 19160483]

Tonikian R, Zhang Y, Boone C, Sidhu SS. Identifying specificity profiles for peptide recognition modules from phage-displayed peptide libraries. Nature protocols. 2007; 2:1368–1386. [PubMed: 17545975]

Torrino S, Visvikis O, Doye A, Boyer L, Stefani C, Munro P, Bertoglio J, Gacon G, Mettouchi A, Lemichez E. The E3 ubiquitin-ligase HACE1 catalyzes the ubiquitylation of active Rac1. Developmental cell. 2011; 21:959–965. [PubMed: 22036506]

Verdecia MA, Joazeiro CA, Wells NJ, Ferrer JL, Bowman ME, Hunter T, Noel JP. Conformational flexibility underlies ubiquitin ligation mediated by the WWP1 HECT domain E3 ligase. Molecular cell. 2003; 11:249–259. [PubMed: 12535537]

Wang HR, Zhang Y, Ozdamar B, Ogunjimi AA, Alexandrova E, Thomsen GH, Wrana JL. Regulation of cell polarity and protrusion formation by targeting RhoA for degradation. Science. 2003; 302:1775–1779. [PubMed: 14657501]

Wang M, Guo L, Wu Q, Zeng T, Lin Q, Qiao Y, Wang Q, Liu M, Zhang X, Ren L, et al. ATR/Chk1/Smurf1 pathway determines cell fate after DNA damage by controlling RhoB abundance. Nature communications. 2014; 5:4901.

Wiesner S, Ogunjimi AA, Wang HR, Rotin D, Sicheri F, Wrana JL, Forman-Kay JD. Autoinhibition of the HECT-type ubiquitin ligase Smurf2 through its C2 domain. Cell. 2007; 130:651–662. [PubMed: 17719543]

Wilson FH, Disse-Nicodeme S, Choate KA, Ishikawa K, Nelson-Williams C, Desitter I, Gunel M, Milford DV, Lipkin GW, Achard JM, et al. Human hypertension caused by mutations in WNK kinases. Science. 2001; 293:1107–1112. [PubMed: 11498583]

Zhang J, Yang PL, Gray NS. Targeting cancer with small molecule kinase inhibitors. Nature reviews. Cancer. 2009; 9:28–39. [PubMed: 19104514]

Zhang W, Sidhu SS. Development of inhibitors in the ubiquitination cascade. FEBS letters. 2014; 588:356–367. [PubMed: 24239534]

Zhang Y, Zhou L, Rouge L, Phillips AH, Lam C, Liu P, Sandoval W, Helgason E, Murray JM, Wertz IE, et al. Conformational stabilization of ubiquitin yields potent and selective inhibitors of USP7. Nature chemical biology. 2013; 9:51–58. [PubMed: 23178935]

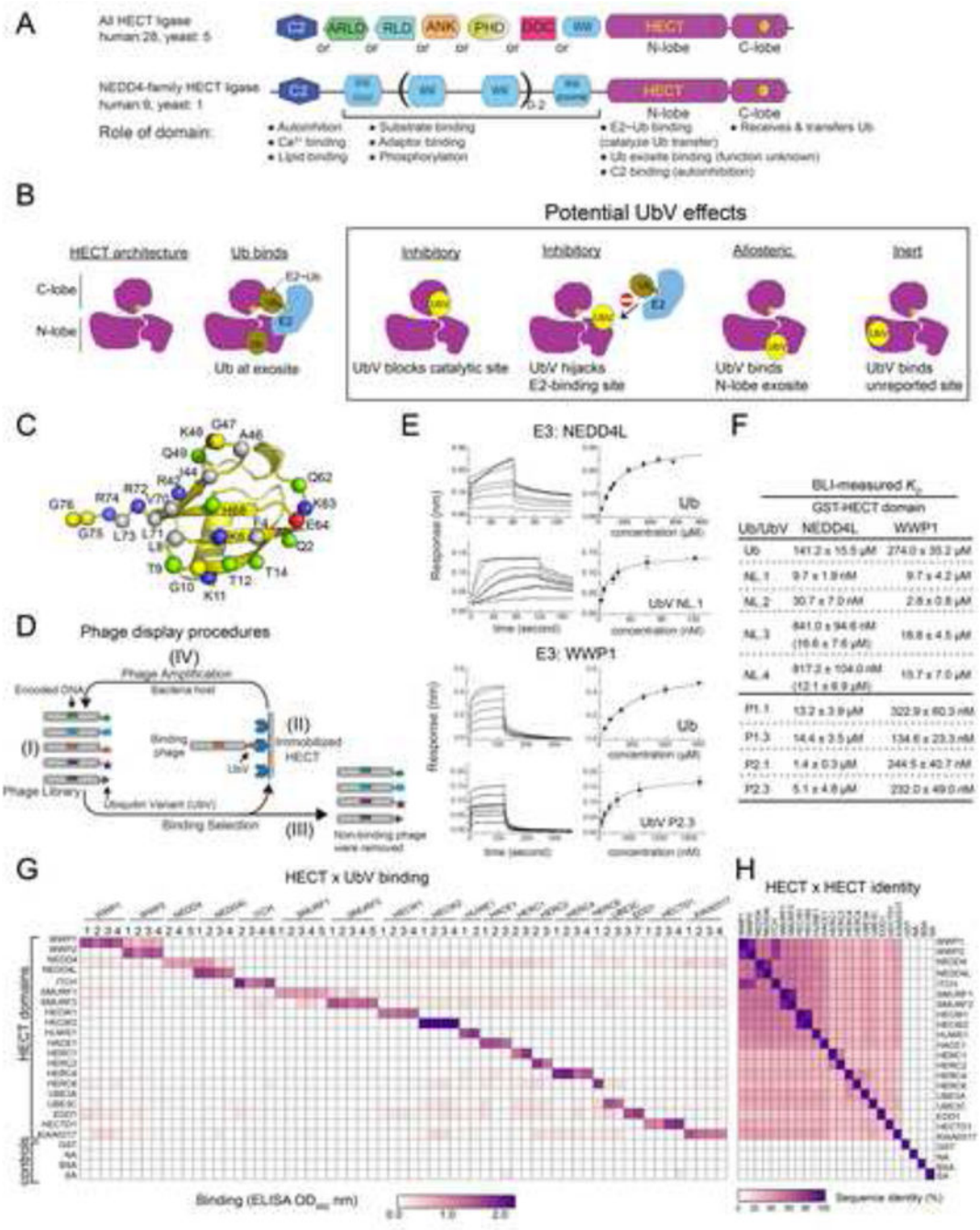

Figure 1. A panel of high affinity ubiquitin variants (UbVs) that bind selectively across the HECT E3 family

(**A**) Schematic diagrams of HECT E3 ligases, with variable N-terminal domains and a conserved C-terminal HECT domain comprised of N- and C-lobes. The variable region of the largest HECT family (NEDD4-family) contains an N-terminal C2 domain and 2–4 WW domains. Domain functions are listed. (**B**) Schematic drawing of HECT sub-domains and known binding interactions with E2~Ub or Ub. Different classes of HECT-UbV binding complexes are anticipated from an unbiased screen. (**C**) Positions subjected to diversification

in the phage-displayed library used to select HECT-binding UbVs. Basic, acidic, polar, hydrophobic and Gly residues are colored blue, red, green, gray and yellow, respectively. (**D**) Phage display selection of UbVs binding to HECT E3 ligases, adapted with modification from (Zhang and Sidhu, 2014). See Experimental Procedures for details. (**E**). Representative sensorgrams and curve fits from binding measured by bio-layer interferometry (BLI), with soluble Ub/UbVs and immobilized GST-HECT domain fusions (NEDD4L and WWP1, 52% sequence identity). Error bars show SEM from two independent measurements. (**F**). Dissociation constants for Ub and UbV binding from titrations in (**E**). NL refers to UbVs selected for binding to NEDD4L, and P1 and P2 refer to UbVs selected for binding to WWP1 or WWP2, respectively. Weak affinities for second sites are in parentheses. (**G**) The binding specificities of phage-displayed UbVs *(x-axis*, detailed sequence information in Table S2) are shown across the HECT family *(y-axis)*, as assessed by phage ELISA. Cognate HECT E3s are noted on top of individual graphs. Sub-saturating concentrations of phage were added to immobilized proteins as indicated (20 HECT domains and 4 control proteins, GST, BSA, and NA (neutravidin), and SA (streptavidin)). Bound phage were detected by the addition of anti-M13-HRP and colorimetric development of TMB peroxidase substrate. The mean value of absorbance at 450 nm is shaded in a purple gradient (white = 0, purple = 2.2 or greater signal). (**H**). Sequence identity matrix shows conservation amongst the 20 HECT domains, but not negative control proteins shown in (**G**) (white = 0 and purple = 100% identity). See also Figures S1 and S2.

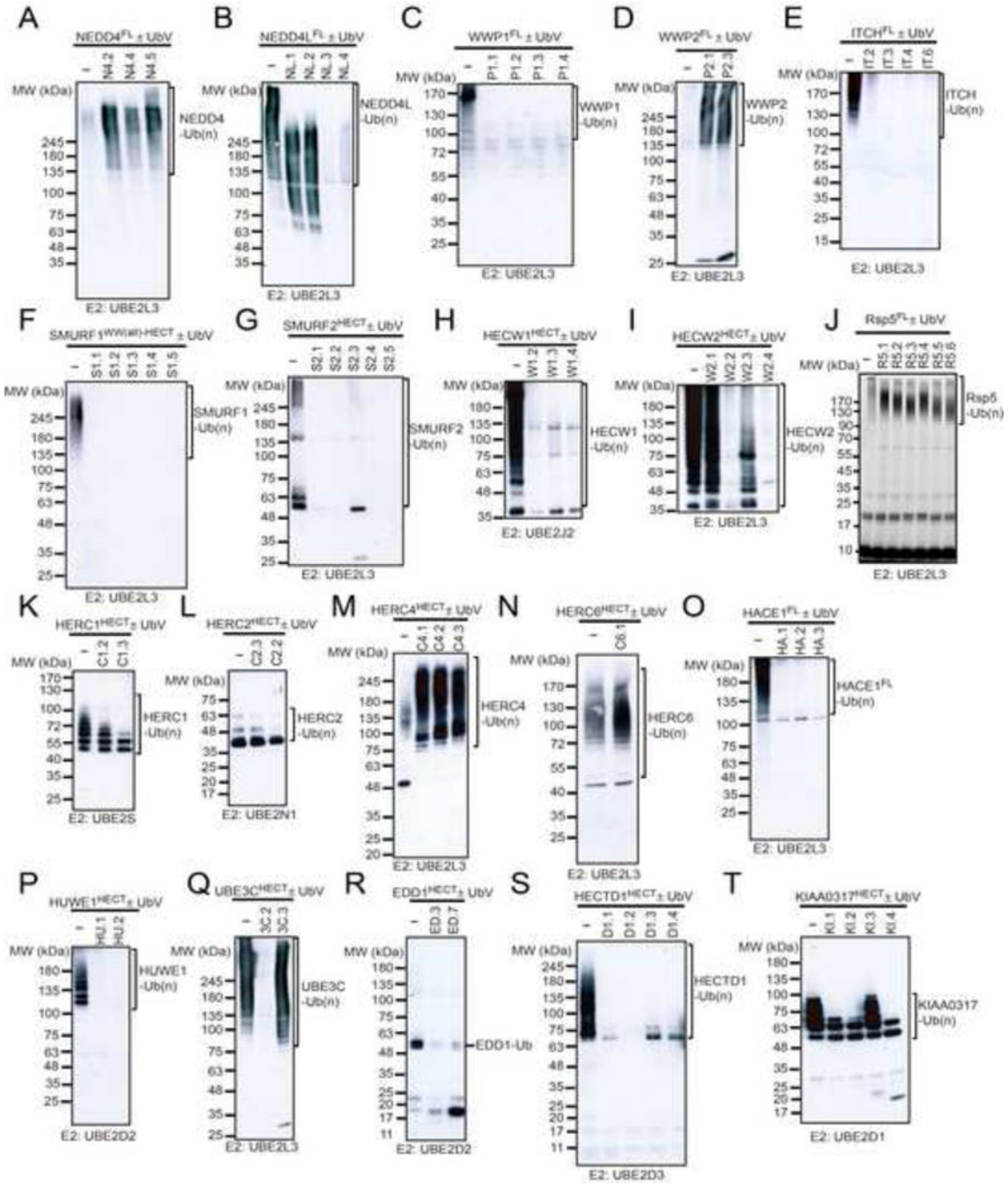

Figure 2. Auto-ubiquitination assay for 20 HECT E3 ligases

(**A**) NEDD4 full-length (NEDD4^{FL}) protein (pre-mixed for 15 min with wt Ub or UbV as indicated) was incubated for 1 hour at room temperature with E1 (UBE1), E2 (UBE2L3), ATP, and Ub. Western blots were probed with an anti-Ub antibody (clone FK2) to detect mono- and polyubiquitinated NEDD4^{FL}. UbVs are not incorporated into chains because their C termini do not contain a di-glycine motif that is required for recognition by the E1 enzyme. (**B**–**T**) Analysis of *in vitro* reactions to detect auto-ubiquitination of other members of the HECT E3 family under conditions described in (**A**). The following HECT E3s were

analyzed: (**B**) NEDD4^{FL},(**C**) WWP1^{FL}, (**D**) WWP2^{FL} (**E**) ITCH^{FL}, (**F**) SMURF1$^{WW(all)\text{-}HECT}$, (**G**) SMURF2 HECT domain, (**H**) HECW1 HECT domain (UBE2J2 was used as E2), (**I**) HECW2 HECT domain, (**J**) Rsp5^{FL}, (**K**) HERC1 HECT domain (UBE2S was used as E2), (**L**) HERC2 HECT domain (UBE2N1 was used as E2), (**M**) HERC4 HECT domain (UBE2L3 was used as E2), (**N**) HERC6 HECT domain (UBE2L3 was used as E2), (**O**) HACE1^{FL} (UBE2L3 was used as E2), (**P**) HUWE1 HECT domain (UBE2D2 was used as E2), (**Q**) UBE3C HECT domain (UBE2L3 was used as E2), (**R**) EDD1 HECT domain, (UBE2D2 was used as E2), (**S**) HECTD1 HECT domain, (UBE2D3 was used as E2), and (**T**) KIAA0317 HECT domain. (UBE2D1 was used as E2). E2s were selected according to published work (Sheng et al., 2012).

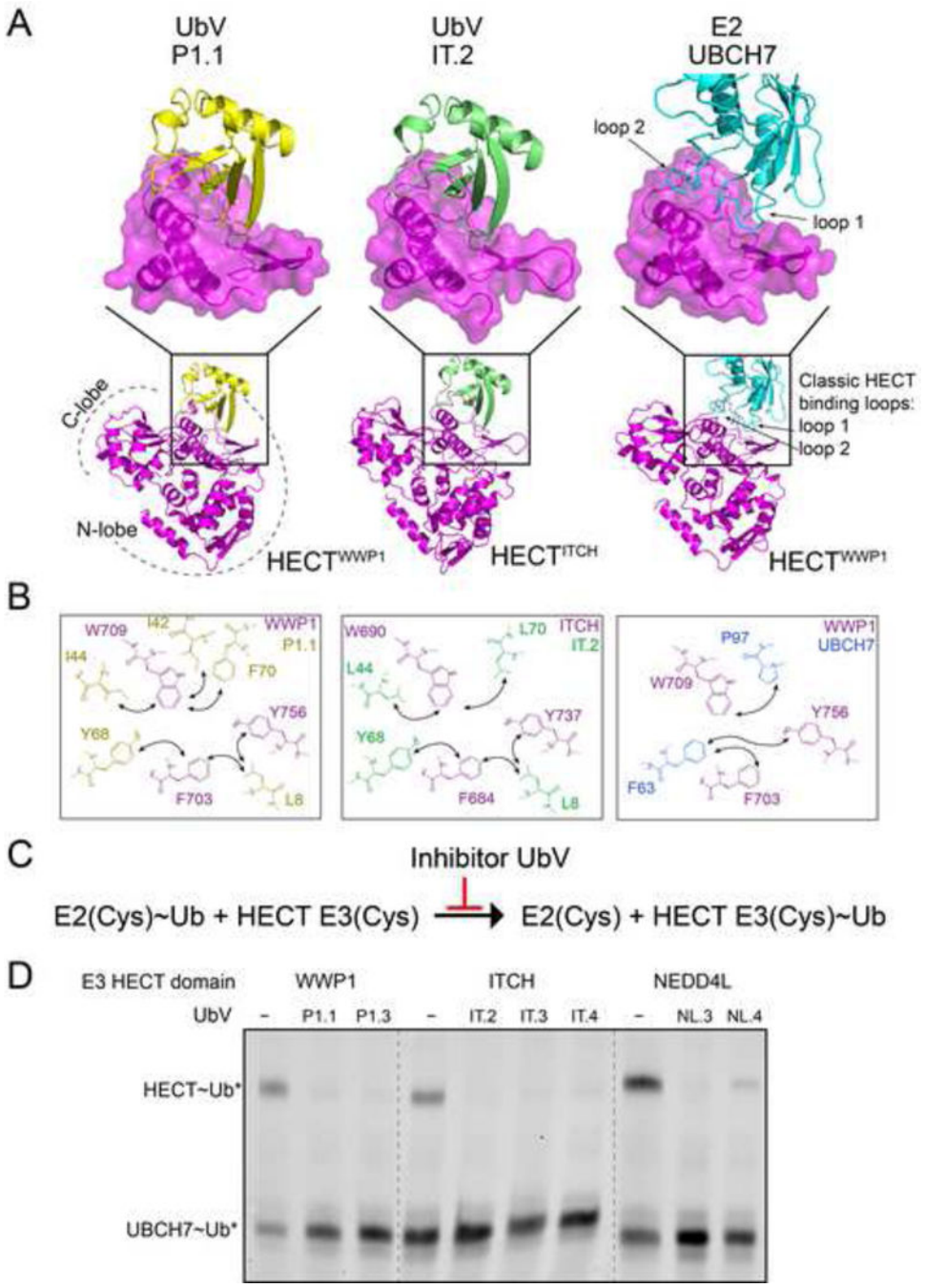

Figure 3. UbV inhibitors block the E2-binding site

(**A**) Crystal structures of UbV P1.1 and IT.2 in complex with the HECT domains of WWP1 or ITCH, shown beside a complex of the WWP1 HECT domain and E2 enzyme UBCH7. Structures are shown aligned by the highlighted E2-binding subdomain. Details of interactions are in Figure S3. (**B**) UbV hydrophobic patch residues hijack the canonical binding site for F63 and P97 from the E2 UBCH7 (Huang et al., 1999). (**C**) Schematic view of HECT E3 reaction involving E2, binding of which would be blocked by UbVs. (**D**).

Phosphorimager data from pulse-chase assay showing transfer of fluorescent Ub to indicated E3 HECT domain, showing effects of selected inhibitory UbVs. See also Figure S3.

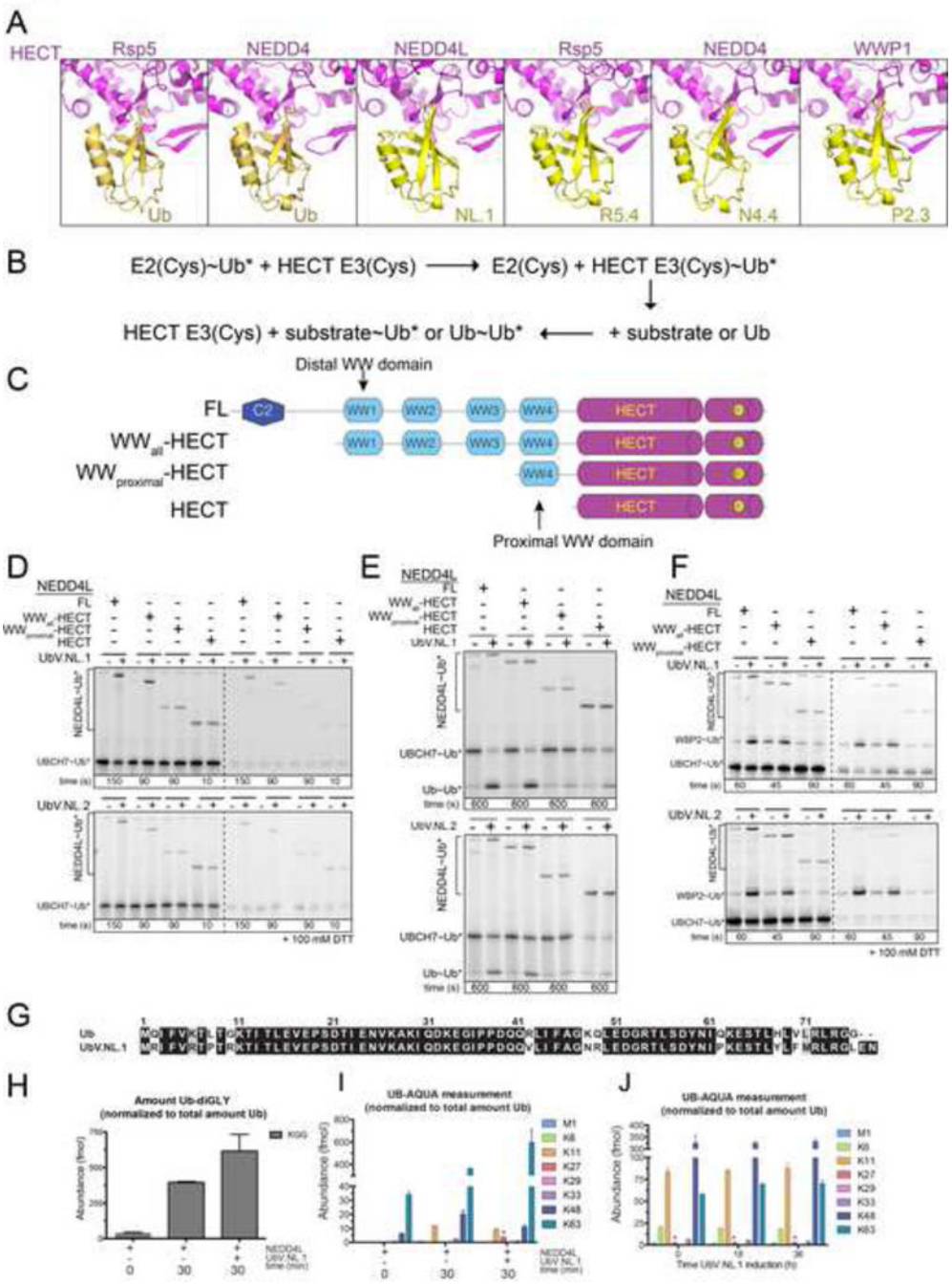

Figure 4. UbV activators bind to the N-lobe exosite

(**A**) Close-up view of crystal structures of indicated HECT-Ub and HECT-UbV complexes, with HECT domains in magenta, Ub in olive and UbVs in yellow. Details of interactions are in Figure S4. (**B**) Scheme of pulse-chase reactions. A thioester-bonded E2~Ub intermediate was enzymatically generated using E1, E2 UBCH7 and fluorescently-labeled Ub. After quenching formation of the E2~Ub intermediate, various versions of HECT E3s were added either alone, or with the substrate WBP2 or free Ub. Reactions were monitored by following the fluorescent Ub, first in E2~Ub, then in E3~Ub, and where tested ultimately in

substrate~Ub or Ub~Ub products. (**C**) Schematic diagrams of NEDD4L and WWP1 deletion mutants used in assays to define domains (C2, all WW domains, proximal WW domain, and/or catalytic HECT domain) required for UbV modulation of ubiquitination activities. (**D**) Pulse-chase reactions testing effects of UbVs (Top: UbV NL.1, Bottom: UbV NL.2) on NEDD4L-mediated Ub transfer from E2 to E3. Requirements of various E3 domains for UbV modulations were examined with four deletion constructs for each E3. For NEDD4L, the distal WW domains, present in NEDD4L^{FL} and NEDD4L$^{WW(all)\text{-}HECT}$ but not NEDD4L$^{WW(proximal)\text{-}HECT}$, are required for UbV stimulation of catalysis. (**E**) Pulse-chase reactions testing effects of UbVs on free Ub chain formation by NEDD4L, from phosphorimager data monitoring effects of UbVs on fluorescent Ub transfer from an E2 (UBCH7), to the indicated WT or deletion mutant version of NEDD4L, to free Ub. (**F**) Pulse-chase reactions testing effects of UbVs on NEDD4L-mediated Ub transfer from E2 to E3 to substrate. These reactions require the WW domains for substrate recruitment. For NEDD4L, the distal WW domains, present in NEDD4L^{FL} and NEDD4L$^{WW(all)\text{-}HECT}$ but not NEDD4L$^{WW(proximal)\text{-}HECT}$ are required for UbV stimulation of catalysis. (**G**) Sequence alignment of Ub and UbV NL.1. The white letters on a black background indicate identical sequences and the black letters on a grey background indicate similar sequences. Due to sequence identity with UbV NL.1, K27 and K29 linkage of Ub could not be absolutely quantified. (**H–J**) UB-AQUA proteomics of total Ub-diGly (**H**) and individual Ub chain linkage types (**I**) for *in vitro* NEDD4L reaction mixtures (45 min) and the effect of UbV NL. 1. Error bars represent experimental triplicate measurements (± SEM). (**J**) UB-AQUA proteomics of individual Ub chain linkage types measured from whole cell lysate HEK293 cells expressing UbV NL.1 for the time indicated. Error bars represent biological triplicate measurements (± SEM). *: Amount quantified can be from Ub and/or UbV NL.1. See also Figure S4.

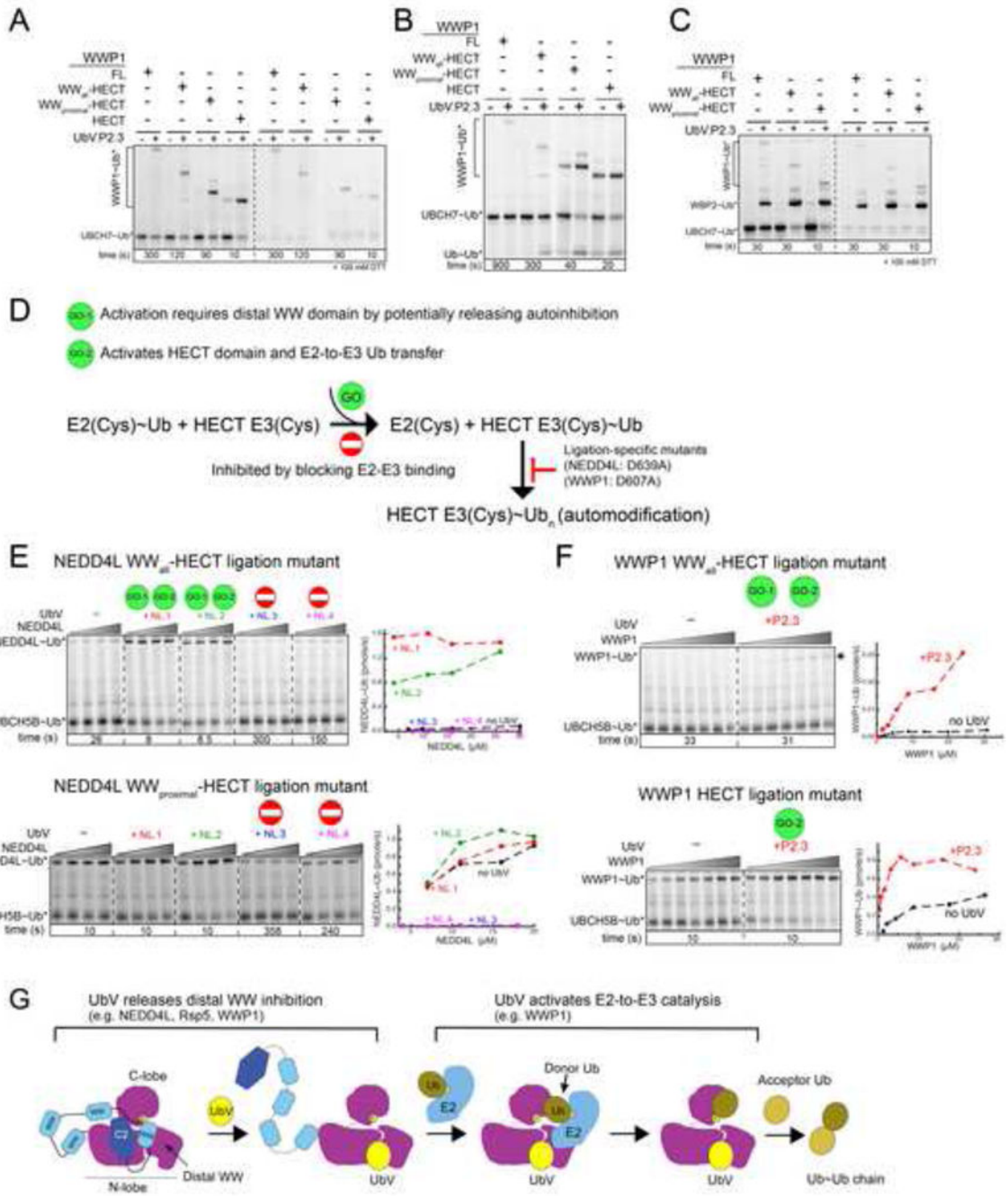

Figure 5. UbVs binding to the N-lobe exosite differentially modulate related HECT E3 ligases

(**A–C**) Same reactions were performed as in Figure 3D–F, except for the HECT E3 WWP1. UbV P2.3 can activate all versions of WWP1 from E2 to E3 then to substrate of Ub~Ub synthesis. (**D**) Schematic of mechanisms by which UbVs activate (GO) or inhibit (STOP) Ub transfer from an E2 to a HECT E3. To prevent HECT E3 autoubiquitination, E3s were mutated with an Ala substitution at a conserved Asp that is dispensable for Ub transfer from E2 to NEDD4-family HECT E3s but that is required for Ub transfer from NEDD4-family HECT E3s to lysines (Kamadurai et al., 2013). (**E**) Roles of distal WW domains in UbV

modulation of Ub transfer from E2 (UBCH5B) to NEDD4L, assayed by titrating UbVs into reactions with versions of NEDD4L harboring all WW domains ($NEDD4L^{WW(all)\text{-}HECT}$) or only the proximal WW domain ($NEDD4L^{WW(proximal)\text{-}HECT}$) in addition to the catalytic HECT domain. The distal WW domains are required for NL.1 and NL.2 to stimulate catalysis, whereas NL.3 and NL.4 inhibit Ub transfer from E2 to both versions of the E3. Note different reaction times used to highlight activation or inhibition. (**F**) Same as (**E**), but for the E3 WWP1 and an activating UbV. Notably, for WWP1, even the isolated catalytic HECT domain alone is stimulated by the UbV in these reactions. (**G**) Models for different steps in Ub chain formation affected by UbVs binding to various NEDD4-family HECT E3s. For NEDD4L and Rsp5, UbV stimulation requires distal WW domains, potentially by releasing their autoinhibition. For WWP1, UbV stimulation only requires the HECT domain, which may be conformationally stabilized by UbV binding. See also Figures S4, S5, and S6.

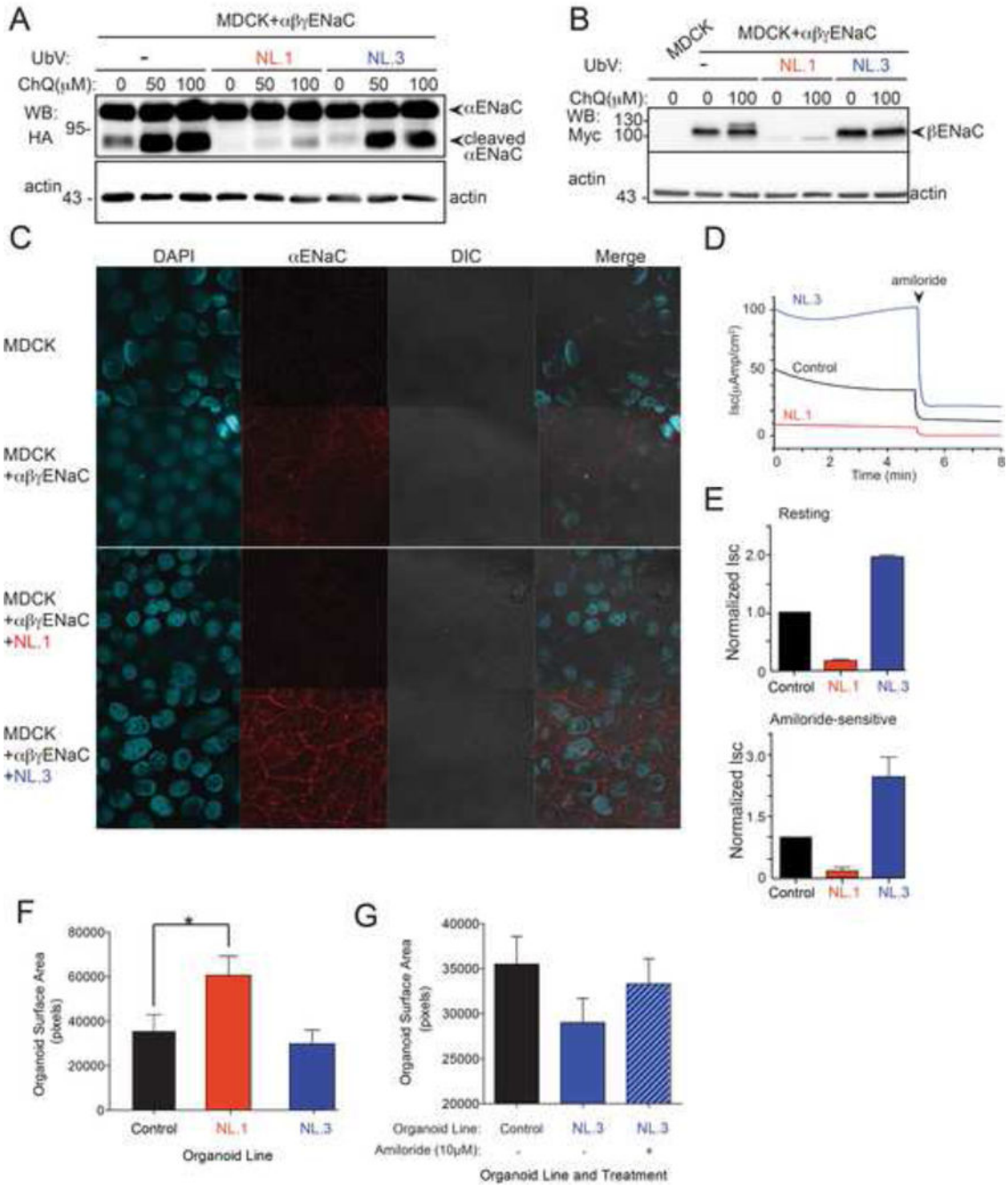

Figure 6. UbVs modulate NEDD4L functions in cells and intestinal organoids (mini-guts)

(**A–B**) Western blot analysis of protein levels of HA-tagged αENaC (**A**) and Myc-tagged βENaC (**B**) (in MDCK cells stably expressing α3xHA, βmyc,T7 and γFLAG-ENaC) with NEDD4L UbV NL.1 or NL.3 (or no UbV) in cells treated (or not) with the indicated concentrations of the lysosomal inhibitor chloroquine (ChQ). Actin blots are shown as loading control. Reduced levels of cleaved αENaC (the active form of αENaC) and βENaC were observed with the expression of NL.1 but not NL.3. (**C**) Immunofluorescence analysis of cell surface ENaC in MDCK cells (stably expressing tagged α, β, and γENaC,

αβγENaC) co-expressing either UbV NL.1 or NL.3. Non-permeablized cells were stained for αENaC with antibodies directed to its ectodomain. Cells were then permeabilized and stained for DAPI (nucleus). (**D**) ENaC function (Isc) analyzed in Ussing chambers in the above MDCK cells stably expressing tagged αβγENaC alone or together with NL.1 or NL.3. The traces from one representative experiment (arrow: apical addition of the ENaC inhibitor amiloride, 10 μM) are shown. (**E**) Summary of 3 separate experiments (mean ± SEM) of resting Isc or amiloride-sensitive Isc as described in (**D**). (**F–G**) Quantification of surface area (in pixels) of control intestinal (distal colon) organoids (GFP-transduced) or organoids expression ubiquitin variant (NL.1 or NL.3), 7 days after seeding. Histogram bars represent mean ± SEM. N = 30–40 organoids per condition. Pixel count to surface area ratio is 1 pixel to 0.78 μm^2. In (**F**), Statistical analysis demonstrated a significant difference in surface area between the control and NL.1-expressing organoids (*t*-test, $p < 0.05$). In (**G**), NL.3-expressed organoids were incubated with or without amiloride (10 μM) for 30 min followed by analysis of surface area by microscopy. See also Figure S7.

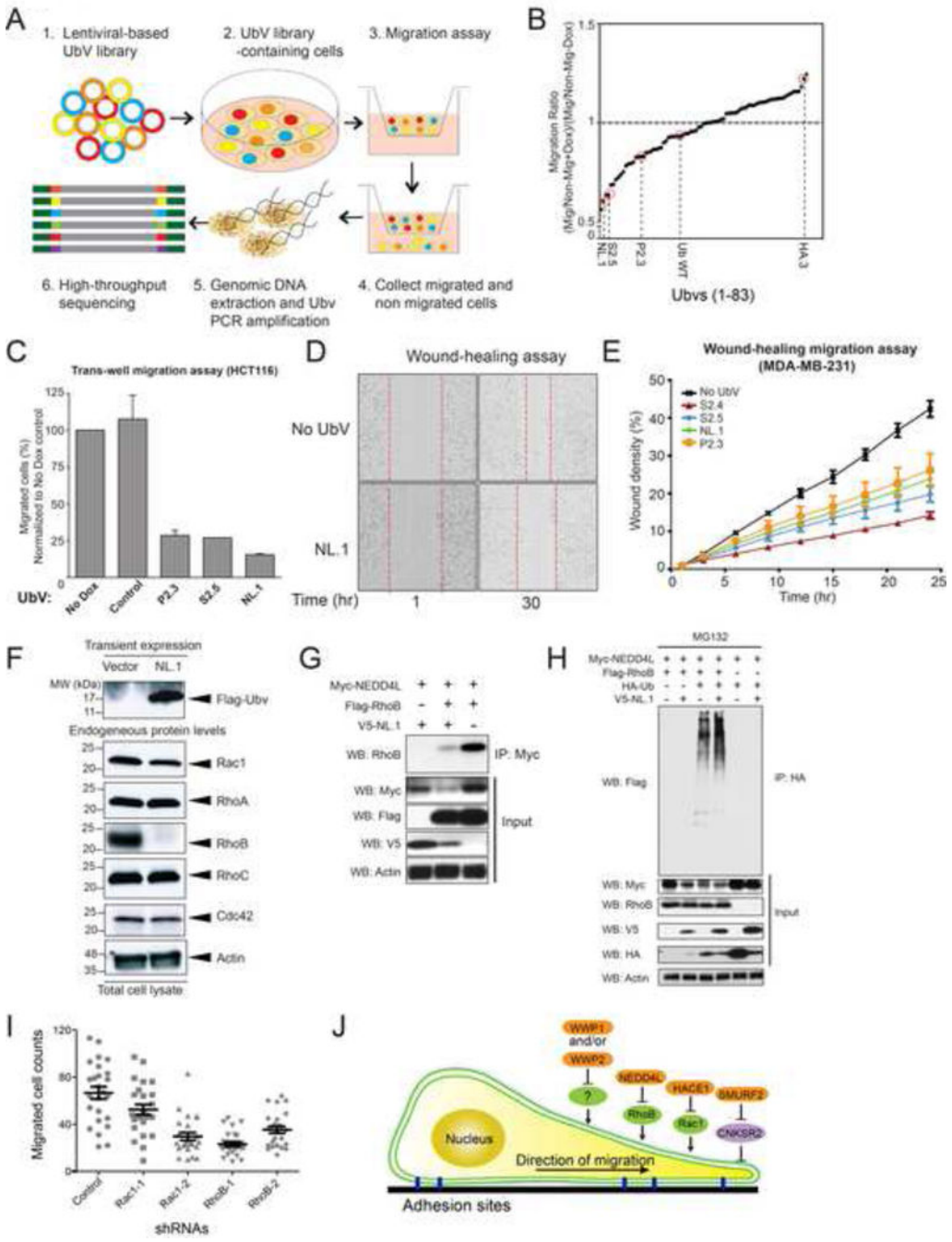

Figure 7. UbVs reveal new functions of HECT E3s in cell migration

(**A**) Schematic representation of the HECT UbV lentiviral library screens for the identification of UbVs affecting cell migration (see Experimental Procedures for details). (**B**) Ranking by migration ratio of 83 UbVs from two independent pooled UbV lentivirus screens examining cell migration in HCT116 cells using a trans-well assay. UbVs discussed in the text are circled. (**C**) Quantitation of migrated HCT116 cells (%) stably expressing control Ub and indicated UbVs using the trans-well assay. The data were presented as the mean ± SEM (N = 3) normalized to non-Dox treatment control. (**D**–**E**) Wound healing assay

was performed to examine the effect of indicated UbVs on cell migration efficiency. Representative photos of scratch wound closure with and without expression of NL.1 are shown in (**D**). (**E**) Quantitation of relative wound density closure after scratch in MDA-MB-231 cells stably expressing indicated UbVs (no UbV as control). The data are presented as the mean ± SEM (N = 3). (**F**) Expression of NL.1 destabilizes RhoB. Whole-cell extracts from HCT116 cells with transient expression of vector or FLAG-tagged NL.1 were subjected to western blotting using the indicated antibodies. (**G**–**H**) NEDD4L immunoprecipitated (**G**) and ubiquitinated RhoB in cells (**H**). NL.1 stimulated the activity of NEDD4L (**H**). HCT116 cells were transfected with constructs encoding HA-Ub, Myc-NEDD4L, FLAG-RhoB, and UbV NL.1. Whole cell lysates were subjected to immunoprecipitation (IP) with Myc (**G**) or FLAG (**H**) antibody and followed by western blotting using the indicated antibodies. Cell lysates were also immunoblotted with the indicated antibodies to monitor expression levels. (**I**) RhoB is required for cell migration of HCT116 cells. Quantitation of migrated HCT116 cells expressing control shRNA or two different shRNAs targeting Rac1 or RhoB. Scatter blots of mean migrate cell counts from 3 independent experiments were shown. (**J**) Schematic illustration of the roles of HECT E3 ligases in regulation of cell migration. UbV inhibitors confirmed that SMURF2 promotes and HACE1 inhibits cell migration, presumably through ubiquitination of CNKSR2 or Rac1, respectively. In addition, UbV activators revealed that NEDD4L inhibits cell migration by ubiquitination of RhoB and activation of WWP1 and/or WWP2 also leads to decreased cell migration. See also Figure S7.

Table 1

Structure data collection and refinement statistics.

Protein complexes	**ITCH^{HECT}-IT.2**	**NEDD4^{HECT}-N4.4**	**WWP1^{HECT}-P1.1**	**Rsp5^{HECT}-R5.4**	**NEDD4L^{HECT}-NL.1**	**WWP1^{HECT}-P2.3-UBCH7**
PDB ID	5C7M	5C7J	5HPS	5HPL	5HPK	5HPT
Data collection						
Beam line	APS 19-ID	APS 19-ID	NECAT-24-ID-C	NECAT-24-ID-C	SERCAT-22-ID	NECAT-24-ID-E
Wavelength (Å)	0.97899	0.97918	0.9791	0.9792	0.9792	0.9791
Crystals	Native	Native	Native	Native	Native	SetMet
Unit cell parameters						
Space group	P 3 2 1	P 3_2	C 1 2 1	P 1 2_1 1	P 4 2_1 2	P 2_1 2_1 2_1
a, *b*, *c* (Å)	121.115, 121.115, 85.547	139.867, 139.867, 59.386	207.9, 44.91, 60.2	72.486, 92.352, 82.161	151.306, 151.306, 85.922	114.005, 118.897, 158.663
α, β, γ (°)	90, 90,120	90, 90,120	90, 96.07, 90	90, 101.6, 90	90, 90, 90	90, 90, 90
Resolution (Å)	49.43-3.03	50.00-3.00	103.5-2.05	80.48-2.31	45.976-2.431	95.15-2.84
Measured reflections	1,286,517	725,669	130,097	151,799	556,930	342,597
Unique reflections	14277 (1343)	26023 (2663)	34,664 (3461)	45787 (4593)	38009 (3757)	51506 (5066)
Completeness (%)	99.5 (96.97)	99.99 (100.00)	98.65 (99.3)	98.17 (98.58)	99.79 (99.89)	99.86 (99.74)
Rmerge	0.094 (0.908)	0.071 (0.979)	0.0615 (0.544)	0.134 (0.9418)	0.135 (0.89)	0.1414 (1.359)
Overall $I/\sigma I$	61.41 (4.4)	34.75 (2.06)	12.96 (2.5)	7.72 (1.41)	17.36 (1.56)	15.7 (1.73)
Multiplicity	18.1 (18.5)	7.6 (7.8)	3.8 (3.8)	3.3 (3.4)	12.1 (2.94)	6.7 (6.7)
Wilson B-factor	96.69	97.47	37.42	38.88	51.26	67.3
Refinement						
Resolution (Å)	49.43-3.03 (3.143-3.034)	50.00-3.00 (3.107-3.0)	103.5-2.05 (2.12-2.05)	80.48-2.31 (2.393-2.31)	35.66-2.431 (2.4919-2.431)	95.15-2.84 (2.942-2.84)
R_{work}/R_{free}	0.2537/0.2969	0.2272/0.2766	0.2159/0.2643	0.1942/0.2499	0.2114/0.2268	0.2184/0.2374
Rmsd bond lengths (Å)	0.008	0.007	0.01	0.012	0.011	0.011
Rmsd bond angles (°)	0.83	1.116	1.28	1.354	1.207	1.612
Number of protein atoms	3868	7157	3793	7464	3749	13524
Number of water atoms	3	4	70	285	131	5
B factor-average	104.6	100.8	51	45.5	53	86.7

Protein complexes	ITCH^{HECT}-IT.2	NEDD4^{HECT}-N4.4	WWP1^{HECT}-P1.1	Rsp5^{HECT}-R5.4	NEDD4L^{HECT}-NL.1	WWP1^{HECT}-P2.3-UBCH7
B factor-Protein	104.6	100.8	51	45.6	53.2	86.7
Ramachandran statistics (Molprobity)						
Preferred (%)	97.02	96.9	95.24	97.87	97.08	94.85
Allowed (%)	2.96	3.1	4.76	2.13	2.92	4.96
Disallowed (%)	0	0	0	0	0	0.19
Clash score	0.14	1.41	8.25	4.27	3.77	15.18

Statistics for the highest-resolution shell are shown in parentheses.